ISSN: 2357- 0954
DOI:10.21608/EJMTC.2024.321077.1287

# An efficient approach to mitigate the effect of antenna steering in SAR images by using platform navigation data

Original Article

**Ahmed Salah ELBohy[1], Ashraf Khaled Helmy[2], Ahmed S. Mashaly[1], Ahmed A. Azouz[1]**

[1]Avionics Department, Military Technical College, [2]National Authority for Remote Sensing and Space Sciences, Cairo, Egypt

**Keywords:**

Synthetic aperture radar (SAR), SAR image formation chirp scaling algorithm (CSA), Sentinel-1 level-0, Blackfill, Entropy.

**Corresponding Author:**

Ahmed Salah ELBohy, Avionics Department, Military Technical College, Cairo, Egypt, **Tel.:** 01006044501, **Email:**a.bohy4phd@gmail.com

***Abstract***

This research paper proposes a novel technique to overcome common challenges in synthetic aperture radar (SAR) imaging, such as the effects of shadows, layover, and multipath interference. The key innovation of the proposed approach lies in two main contributions. First, the strategic use of navigation data to compensate for antenna steering, which introduces irregularities in the missing data regions of SAR images. The technique can effectively mitigate the impact of the aforementioned SAR imaging artifacts. Second, the proposed scheme results indicate due to the integration of digital signal processing (DSP) methods played a crucial role in enabling efficient and effective remedy steps within the image formation algorithm preprocessing. This combined approach is based on platform navigation data powered by DSP when followed by a chirp-scaling algorithm (CSA), one of the most powerful SAR image formation algorithms. This approach when applied to real-world data from the Sentinel-1 satellite has yielded impressive and unprecedented results in compensating the antenna steering and mitigating the backfill, producing reconstructed images that closely resemble the original Sentinel-1 SAR products. To comprehensively validate the performance of the proposed technique, the reconstructed images were assessed against the reference Sentinel-1 data using a suite of established objective metrics, including entropy, contrast, sharpness, Mean Opinion Score (MOS), and structural similarity index measure (SSIM).These quantitative analyses conclusively confirmed the efficacy of the new method in enhancing the overall fidelity and visual quality of SAR imagery.This is very clear as the degree of similarity was recorded on average as (98.4%) and obtained score on the standard scale of MOS is (4.82 out of 5).

## 1. INTRODUCTION

Synthetic Aperture Radar is a remote sensing technology that uses radar to create high-resolution images of the Earth's surface. However, due to various factors such as sensor limitations or environmental conditions[1], SAR images can sometimes have missing or incomplete data, resulting in areas of the image appearing. SAR blackfill refers to a technique used to fill in missing or corrupted data in SAR images

Blackfill algorithms are employed to estimate the missing or corrupted data and fill in the black regions with plausible information. These algorithms are designed to exploit the statistical properties of the surrounding image data to make informed predictions about the missing values. They often utilize techniques such as interpolation, filtering, or statistical modeling to estimate the missing data.

The goal of SAR blackfill is to produce visually coherent and continuous images by reducing the impact of missing or corrupted data. This is particularly important for applications that require accurate interpretation and analysis of SAR imagery, such as land cover mapping, change detection, or target detection[2].

Various SAR blackfill algorithms have been developed, including simple techniques like linear interpolation or more advanced approaches like adaptive filtering or model-based methods. The choice of algorithm depends on the specific characteristics of the missing data and the desired level of accuracy.

It is worth noting that SAR blackfill is an active area of research, and new algorithms and techniques are continually being developed to improve the quality of SAR imagery and address the challenges associated with missing or corrupted dataeither by man intervention or using artificial intelligence.

The Terrain Observation with Progressive Scans (TOPS) SAR imaging mode is characterized by a constant rate of azimuth beam steering from the aft to the fore direction. This approach differs from the Scan SAR mode, as it ensures that all ground targets are observed by the entire azimuth antenna pattern[3]. Consequently, this eliminates the scalloping effect and maintains constant azimuth ambiguities and signal-to-noise ratio (SNR) along the azimuth direction. However, the tradeoff is that the rapid azimuth beam steering reduces the target dwell time, resulting in a lower spatial resolution in the azimuth dimension[4].

The Sentinel-1 satellite employs a roll-steering mode, which introduces an additional roll angle as a function of latitude. This compensates for changes in the satellite's altitude around the orbit due to the shape of the geoid, thereby maintaining a specific, quasi-constant slant range for each SAR imaging mode. This enables the use of a single pulse repetition frequency (PRF) per swath or sub-swath around the orbit. Additionally, Sentinel-1 operates in the total zero-Doppler steering mode, which accounts for the effects of Earth rotation by applying yaw and pitch adjustments around the orbit. The goal of this approach is to achieve Doppler centroid frequencies close to zero hertz [5].

Although Sentinel-1 owns an almost continuous azimuth steering which allows for a perfect compensation at raw data level. Nevertheless, the relatively high azimuth steering may impose noticeable variation in the Doppler centroid as a function of range and/or topography[6,7].

Therefore, we may have an issue related to the movement of the satellite and the angle of the antenna, with its ability to continue following the target or scene area. Missing or corrupted data due to this antenna steering may introduce an error causing shadows, object duplication, or black gap in the image[8-11].

The scalloping imposed by the electronic antenna steering can precisely be corrected using the proposed algorithm, whose backbone is navigation data and digital signal processing (DSP).

Observations of the imagery data reveal the presence of distinct distortions occurring within a specific vertical space in certain images. These distortions tend to remain aligned along the same vertical line or group of vertical lines if they manifest in multiple locations across the image.

Investigation of this phenomenon, building upon previous research by the authors to decode the initial Sentinel-1 satellite data[8], has provided insights into the underlying cause of these distortions. The vertical intervals corresponding to the distortions have been found to coincide with the timing and positioning of the antenna movements within the SAR system. These antenna adjustments are necessary to maintain target tracking as the carrier platform undergoes motion.

The identification of this relationship between the observed distortions and the antenna steering dynamics offers a potential avenue for mitigating these artifacts through appropriate compensatory measures in the image formation process.

The Sentinel-1 SLC products consist of one image per sub-swath, where each sub-swath image is composed of a series of bursts. Each burst has been individually focused and processed as a separate SLC image[1,8]. These individually focused complex burst images are then included in azimuth-time order into a single sub-swath image, with backfill demarcation between the bursts. Due to the single natural azimuth look inherent in the data, the imaged ground area of adjacent bursts will only marginally overlap in the azimuth dimension, just enough to provide contiguous ground coverage.

The images for all bursts in all sub-swaths of the SLC products are resampled to a common pixel spacing grid in both the range and azimuth dimensions. This burst synchronization processing is phase-preserving this is valid under the assumption of SAR platform remains fixed while delivering one pulse and receiving the scattered before changing its position, known as the stop-go model, which is applicable for the chirp scaling algorithm[9,10]. However, during platform movement, the antenna steering required to cover the ground target may introduce phase errors, which can result in shadows, target replicas, or black gaps in the imagery.

The data dissemination and circulation function is responsible for delivering the Global Monitoring for Environment and Security (GMES) Sentinel-1 products to users, typically through electronic server access (e.g., online data provision). This process requires specific algorithms to deal with the effects of the antenna steering rate and the Doppler centroid rate due to the steering. The required azimuth pre-and post-processing of the data includes de-ramping of the data prior to Doppler centroid estimation, azimuth ambiguity estimation, and further processing[11].

## 2. Methods and Materials

### 2.1. Methodology Outlines

Image registration is a fundamental process that enables finding correspondences between input images by estimating the necessary transformation matrix to align selected points in the sensed image with their counterparts in the matched image. Feature detection is an essential step in this process, as it facilitates the interpretation and application of image registration techniques across various domains.

Two main approaches exist for image registration: area-based matching (ABM) and feature-based matching (FBM) methods. The ABM approach focuses on ensuring the existence of features, rather than their explicit detection. In contrast, the FBM approach places significant emphasis on the feature detection process itself[12]. While each approach presents unique advantages, they also exhibit distinct disadvantages that can be mitigated by employing the complementary strengths of the other.

Features can be categorized as either global or local. Global features represent the image as a whole, whereas local features capture specific patches or regions of interest. Examples of features include corners, edges, texture, color, and blobs. Global features, though informative, can be limited in their ability to fully characterize an image, necessitating the use of techniques such as segmentation to recover this information[13].

The usage of local features is generally preferred due to their inherent structural stability and informativeness [12]. The process of identifying a set of salient points with specific properties allows for a more robust and distinctive representation of the image content.

While image coregisteration two radar images need to be recalibrated, it is always possible to retrieve fine information relying on precise knowledge of the satellite's orbital parameters and the terrain's topography. These are purely "geometric" approaches. On the other hand, they require a thorough knowledge of the Digital Elevation Model (DEM), the trajectories used to form the images, and how to access them. In the case of airborne data, challenges arise, particularly when dealing with potentially inaccurate trajectory data.

In the proposed case, it appears that we are demonstrating here a signal domain technique akin to coregisteration technique in the image domain; however, this saves time and effort as there is no need to compose these images and then compare them in order to obtain very clear, high-resolution, error-free images. In addition to there is no need to know or even to be familiar of the DEM.

## 2.2 Detailed Mehtod

The Sentinel-1 satellite acquires navigational data that must be downloaded and processed to extract the requisite parameters for subsequent analysis. A well-defined procedure is then implemented to systematically retrieve the complete set of navigational data corresponding to each individual data sample[8].

The next step involves examining the scene area to detect and quantify any spatial shifts that may have occurred. This is accomplished by downloading and parsing the scene echo file, which enables the determination of the shift index based on the sample number.

Finally, the target signal is isolated by removing extraneous data, such as calibration and acknowledgement information, that could unnecessarily burden the computational processing. The target signal is then adjusted by applying a circular shift equal to the detected spatial offset.

The detailed implementation of this workflow is further elucidated in the accompanying flowchart provided by Figure 1 below.

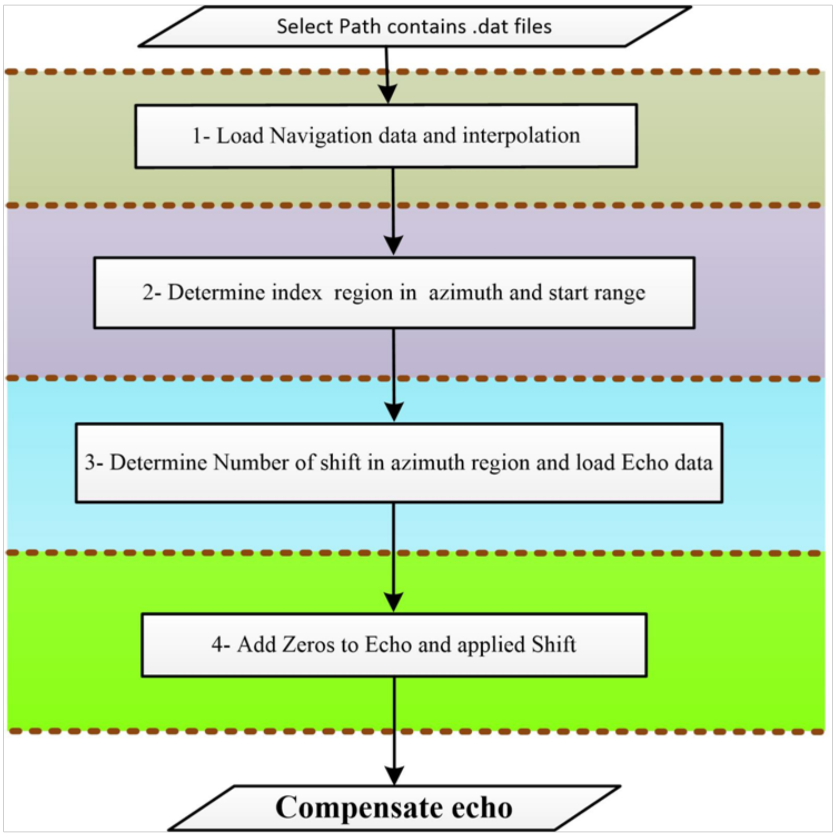


**Fig. 1:** Proposed Algorithm Flowchart

2.2.1. Phases of the Proposed Methodology.

The present study employed a four-step approach to ensure the suitability of the data for the computational resources used and to establish the rhythm of the work. Following this initial, preparation the implementation of the algorithm proceeded through four key stages, as detailed below.

In this section, the basic accelerating method for MATLAB codes is introduced in an intrinsic way. The MATLAB code was optimized without using GPU because the size of data is too large to be saved in GPU memory. The following points are taken in account for SAR processing algorithm:

1- Vectorization: Since MATLAB has the vector/ matrix representation of its data, "vectorization" can help to make your MATLAB codes run faster. The key for vectorization is to minimize the usage of for-loops.

2- Pre-allocation: Resizing an array should be executed before operation since it involves memory deal-location or allocation and value copies each time to resize it. Therefore, pre-allocating the matrices of interest can get a significant speedup. Pre-allocation involves resizing the matrices or arrays that will hold the processed data. That allow avoidance of frequent resizing operations, which can be computationally expensive. This step helps optimize memory usage and can result in more efficient code execution.

3- For-Loop: In many cases, it is inevitable to use a for-loop. As a legacy of FORTRAN, MATLAB stores matrix in a column-major order, where elements of the first column are stored together in order, followed by the elements of the second column, and so forth. Since memory is a linear object and the system caches values with their linear neighbors, the nested loop makes for a matrix, column by column.

4- Parallel for-Loops (parfor): Many applications involve multiple segments of codes, some of which are repetitive. Often you can use for-loops to solve these cases. The ability to execute codes in parallel, on one computer or on a cluster of computers, can significantly improve performance.

The accomplish of this process is based on four phases/ stages:

Phase 1: Load Navigation data and interpolate:

In the first step of the proposed methodology, the relevant index and header files containing metadata about the raw synthetic aperture radar (SAR) data are ingested and parsed. These files typically provide crucial information such as timestamps, sensor parameters, and other metadata necessary for effective understanding and processing of the SAR data. Next, the available navigation data is extracted and leveraged to interpolate and calculate time, position, velocity, and attitude parameters for each individual sample within the SAR data, rather than relying on the coarser one-second granularity. Navigation data, including GPS coordinates and attitude information, is vital for accurately aligning and georeferencing the SAR measurements. Commonly used interpolation techniques, such as linear or spline methods, are employed to estimate these continuous parameters between the discrete navigation data points. Noting that, as the SAR data is initially acquired in Earth-Centered, Earth-Fixed (ECEF) coordinates tied to the Earth's rotation, it is necessary to transform the data to a different, more appropriate coordinate system for further analysis or visualization [9]. In this regard, the data is aligned with a navigation reference frame, which is a crucial preprocessing step prior to subsequent processing and analysis stages.All the mentioned above steps are ilusterated in Figure 2 below.

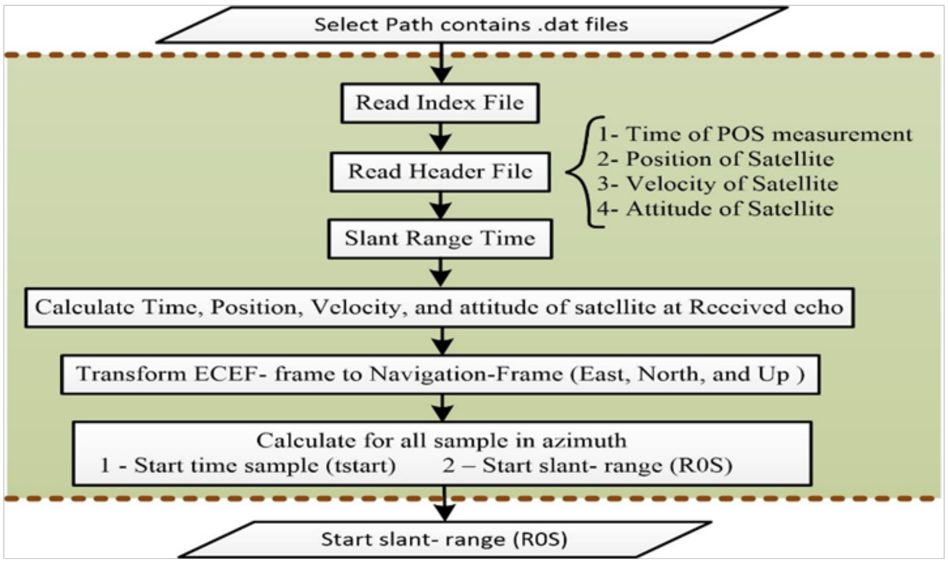


**Fig.. 2:** Load Navigation Data and Intrpolation Process

Accurately calculating the time of receiving echo data (tr) is a crucial parameter in SAR processing. This time depends on several factors, which are illustrated in Figure 3 and can be expressed mathematically as:

$$t_r = PRI * r + SWST + \Delta t_{supp}$$

Where:
- PRI is the pulse repetition interval
- r is the rank, which represents the count of PRIs between the transmitted pulse and its corresponding echo
- SWST is the sampling window start time
- $\Delta t_{supp}$ is the suppressed time, which refers to the transient time of the decimation filter

The pulse repetition interval (PRI) is the time between consecutive radar pulses transmitted by the SAR system. The rank (r) is the ordinal number indicating which received echo pulse corresponds to a particular transmitted pulse. The sampling window start time (SWST) marks the beginning of the time window during which the echo data is recorded[8]. Finally, the suppressed time (Δtsupp) accounts for the transient response of the decimation filter applied to the received signal.

By considering these various temporal parameters, as shown in the time analysis diagram in Figure 3, the precise time of space packet data reception can be calculated using Equation 1. This time calculation is a critical component in the overall SAR image formation and processing

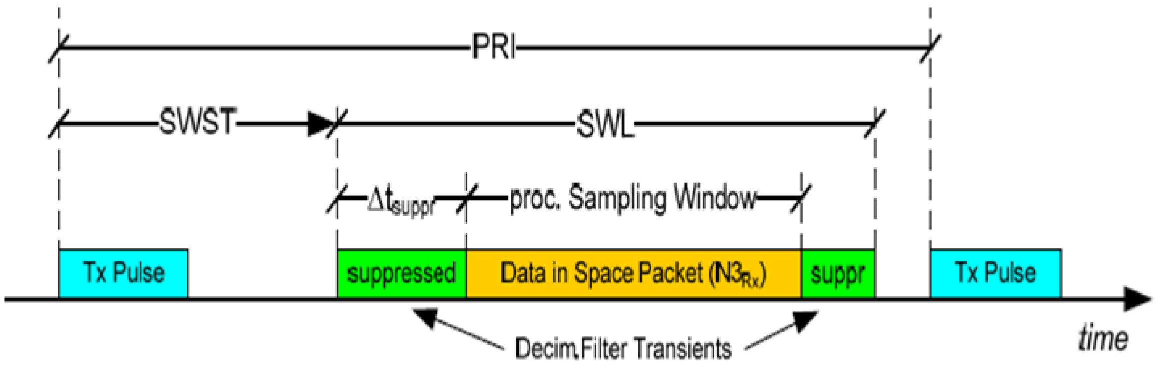


**Fig. 3:** Time analysis of the acquired data in one PRI

## Phase 2: Determine Index and Azimuth start range

The goal of this analysis is to determine the ascending or descending mode of a SAR dataset; this is an important step in the processing of SAR data, as the mode of data acquisition (ascending or descending) can affect the backscatter intensity due to differences in the local incidence angle. That is done via the search for the shortest range (Rmin) in the data, If Rmin is present at the beginning of the data, and we can conclude that the data is in ascending mode. However, if we do not reach Rmin within the data, we continue the search until Rmin is found and then proceed with the data in descending mode. By separating the data into ascending and descending segments, we can ensure that the subsequent processing is compatible with both modes.

The next step is to create an array. The first column contains all the range values up to the point where the shift occurs. The second column contains the range values from that point until the end of the data or the occurrence of another shift and so on, and this step is crucial for making the algorithm general, as SAR datasets can differ in their mode (ascending vs. descending) between acquisitions. Steps of phase 2 clarified by Figure 4.

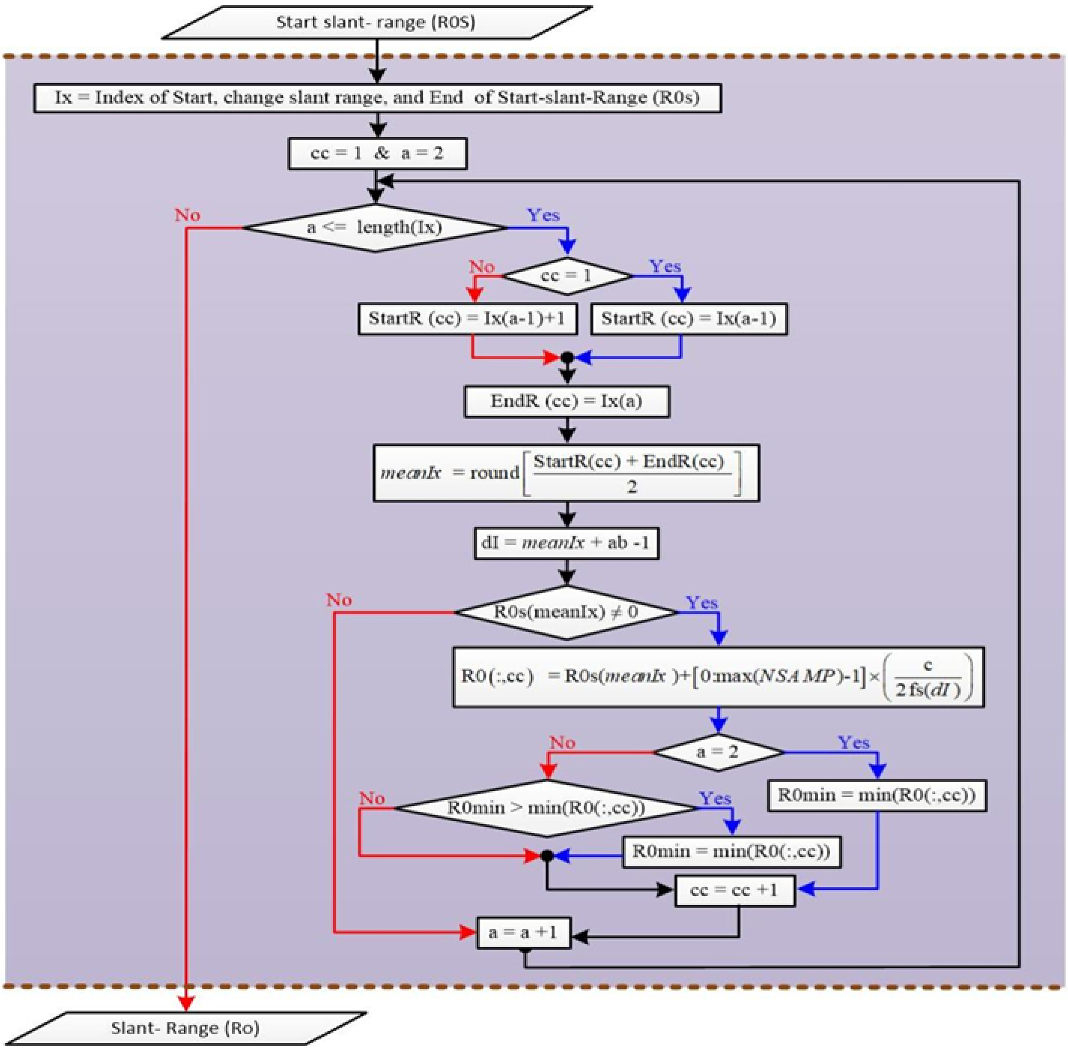


**Fig. 4:** Azimuth Index Determination and Start Range

To implement this, we use a "struct" data structure. "struct" allow the creation of an array of elements with variable size and composition, which is well-suited for handling the potentially varying number and size of the ascending and descending segments in the SAR data. "Struct' is a composite data type in programming, similar to arrays but with named fields instead of indexed elements. This provides a more human-readable and flexible way to organize and access the data, which is particularly beneficial for complex datasets like SAR.

The use of "struct" to store the ascending and descending segments of the SAR data is a key aspect of the generalized algorithm presented here. This approach ensures that the algorithm can handle a wide range of SAR datasets, regardless of their mode of acquisition, and facilitates the subsequent interpolation and compensation steps.

## Phase 3: Determine shift and load echo data

The Echo file contains the raw SAR data, which consists of backscattered radar signals from the target area. This step involves loading the Echo file into memory for further processing and analysis. The raw data acquired from radar imaging systems often contains extraneous information not directly relevant to the formation of the radar image. This extraneous data may include calibration parameters, handshaking protocols, acknowledgment signals, checksums, and other metadata specific to the particular scene area and data exchange timing. Developing a generic data processing algorithm capable of handling this varied supplementary data is a key strength, as it enables the system to robustly accommodate the full range of data types and scene configurations encountered through the radar imaging workflow.

Azimuth shift refers to a change or deviation in the azimuth direction. Azimuth is the angular measurement in the horizontal plane, typically measured clockwise from a reference direction. In this step, you determine if there is a shift in the azimuth direction within the SAR data. If a shift is detected, you identify the index of the shift and calculate the amount of displacement needed to compensate for it. This compensation ensures that the data is correctly aligned and avoids any artifacts or distortions caused by the shift. In this step, calculate the shift between consecutive azimuth samples. By subtracting the azimuth value for each range from the azimuth value for the next range, you can determine the magnitude of the shift in the azimuth direction, Figure 5 below explains the process in a clear manner.This information is useful for further processing or analysis of the SAR data to get the offset (transformation) of the corresponding transformation to compensate for it with the benefit of what was built from struct syntax, which represents a lookup table of values against the index.

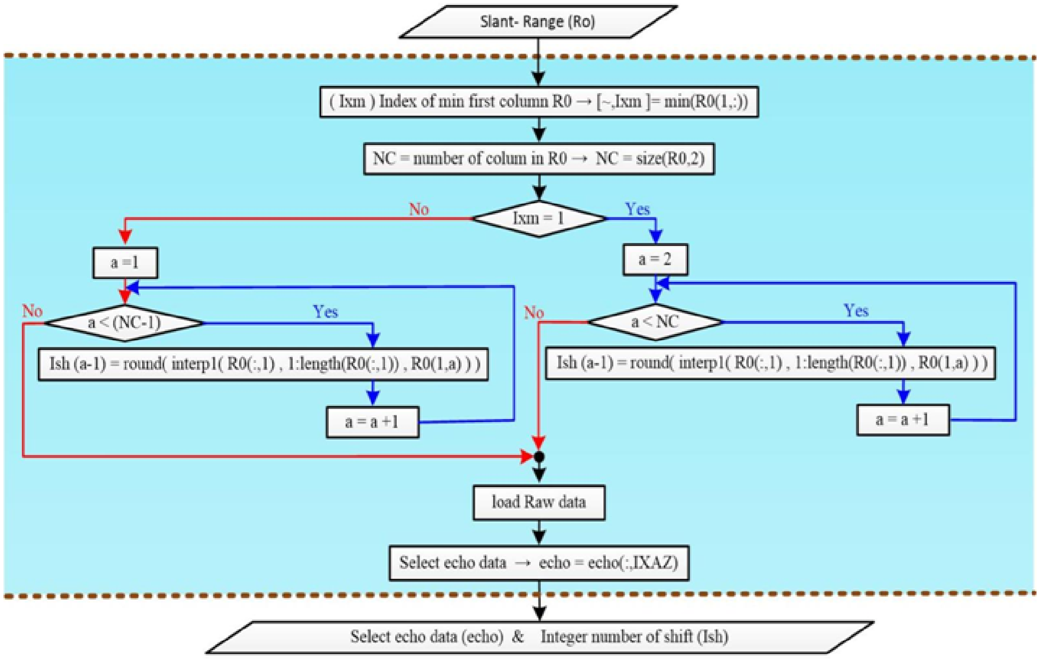


**Fig. 5:** Azimuth Shift Determination and Load Echo Data

A generic model capable of parsing and extracting the relevant imaging data, while properly handling the diverse supplementary information, represents an important advance. This allows the radar image formation process to proceed efficiently without the need for specialized preprocessing or segmentation of the input data stream based on data type or origin. The algorithm's ability to seamlessly integrate the full complement of raw data is a crucial enabler for reliable, high-throughput radar imaging across a variety of operational scenarios and system configurations.

Phase 4: Zero Padding, Circular Shift and compensate for shift : Zero padding involves adding zeros to the echo data in the range direction. This operation is typically performed to achieve a specific data length or format required for subsequent mathematical operations or algorithms. Zero padding can facilitate Fourier transforms Represennt about 70% of SAR processing, spectral analysis, or other signal processing techniques. Circular shifting involves cyclically shifting the elements of an array or matrix in a circular fashion. In the context of SAR data processing, circular shifting is applied to the echo data and helps align the data properly. The amount and direction of the circular shift are often determined based on the calculated shift in the azimuth direction, as shown in Figure 6 below.

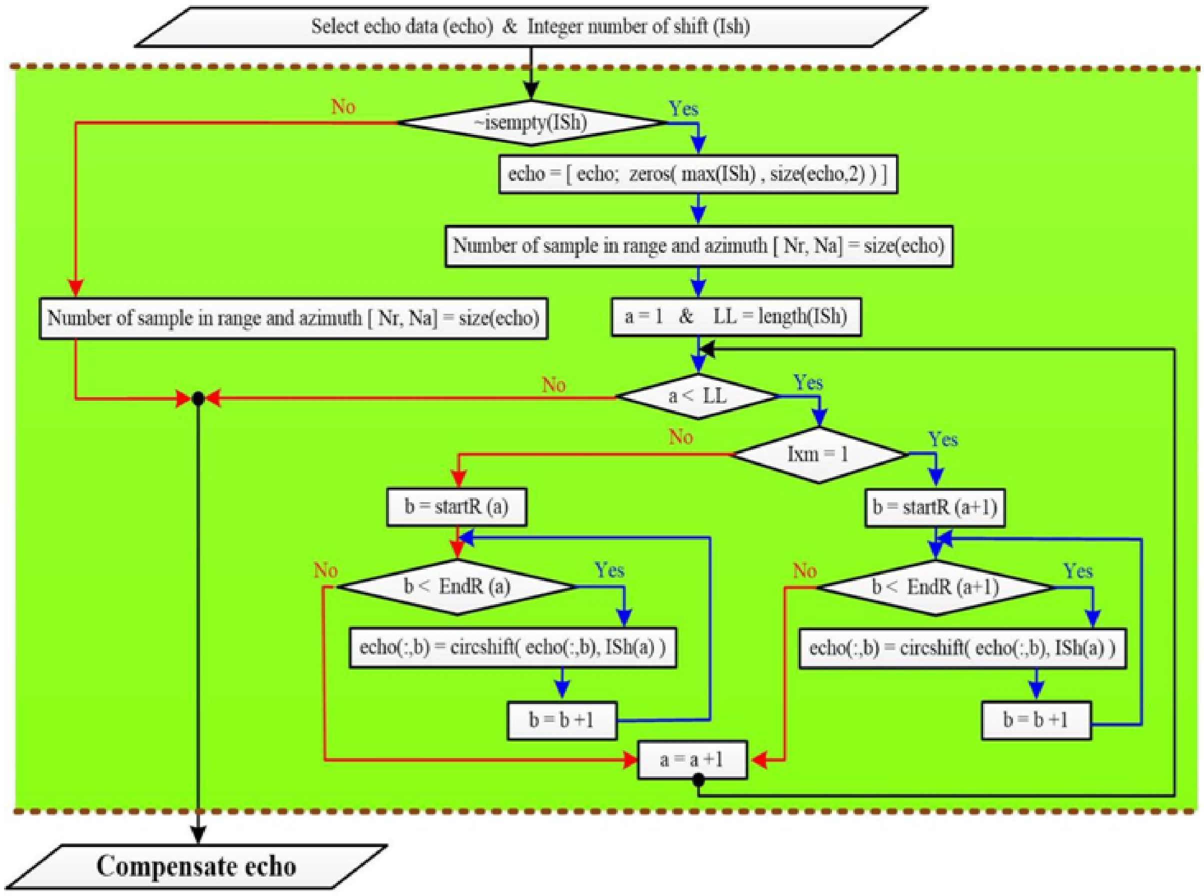


**Fig. 6:** Echo Zero Padding and Shift Compensetion

### 2.2.2.The outstanding algorithm

A generalized algorithmic framework was developed to comprehensively address the range of potential scenarios that may arise. The implemented code accounted for the possibility of any number of spatial shifts, along with arbitrary displacement magnitudes, and whether the Sentinel-1 satellite was operating in ascending or descending orbital modes.

This robust approach ensured the ability to effectively process the data regardless of the specific characteristics of the observed phenomenon. By incorporating flexibility to handle diverse conditions, the program was able to provide a unified solution applicable across the full scope of anticipated use cases. The modular and extensible design of the algorithm enabled it to adapt to evolving requirements or newly encountered situations, thereby maximizing the operational utility and longevity of the data analysis capabilities.

The proposed algorithm represents a preprocessing step that is followed by one of the most significant and powerful image formation algorithm, which was chosen to be a chirp-scaling algorithm due to its many advantages.

Designing a SAR image formation system presents a significant challenge due to the vast array of available algorithms and hardware options. A variety of SAR image formation algorithms exist, including the range-Doppler algorithm (RDA), chirp scaling algorithm (CSA), and back-projection. Each algorithm offers unique advantages and disadvantages in terms of efficiency, processing time, hardware resource requirements, and resulting image quality[14].

The CSA was developed specifically for stripmap SAR to eliminate the need for interpolation in the range cell migration correction (RCMC) technique used in the RDA. The CSA can also handle higher squint angles. The chirp scaling mechanism implements RCMC shifts using phase multiplies instead of interpolation. The main limitation of using the RDA in small laboratories with constrained hardware is the computationally intensive interpolation calculation process [15,16]. In contrast, the CSA addresses this issue by producing high-resolution images with fewer processing steps, reduced hardware resource consumption, and a simpler system implementation compared to the RDA[15]. For all these reasons and features, CSA with its ease and simplicity has become very suitable for use with the Sentinel-1 satellite especially in the cases being studied and in which squint angle may be large with the ability to process all the parameters and variables using a powerful personal computer or a workstation computer.

Conceptually, the proposed algorithm is designed to be used in conjunction with the CSA to construct a well-focused SAR image.

The scheme and algorithm are accomplished using MATLAB 2020b on workstation i7-6820HQ, 32 GByte RAM instead of Sentinel-1 ground station reaching well entropy and contrast for a scene area 80 Km * 200 Km in Netherland centered at Latitude 52.9888° , Longitude 06.0432°.

## 3. Results and Discussion

The scene area under investigation has dimensions of 200 km by 80 km. This large scene has been subdivided into 11 distinct segments, of which five representative segments are presented to cover the different parts of the overall sceneas illusterated in figure 7 a,b,c.

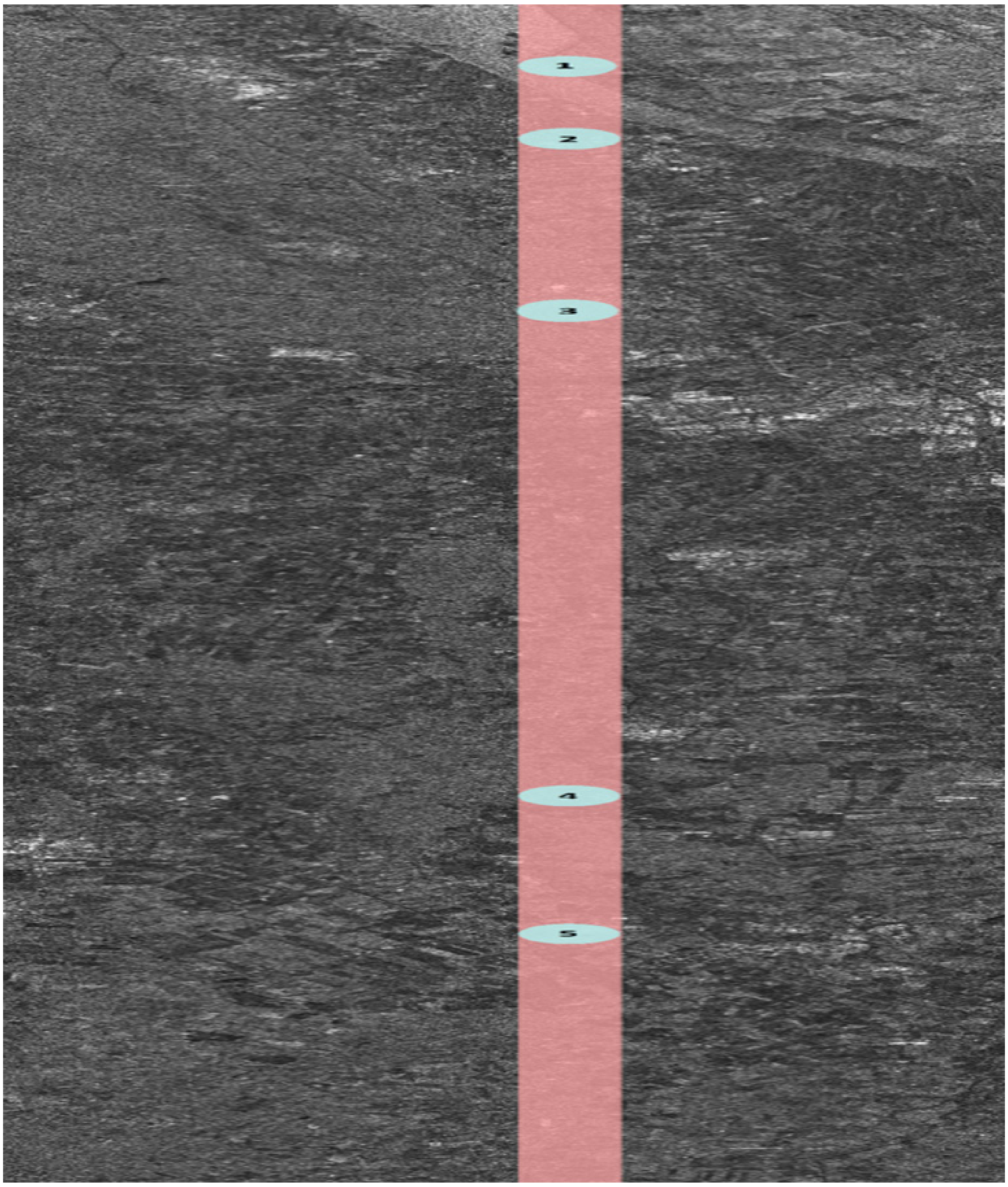


(a)

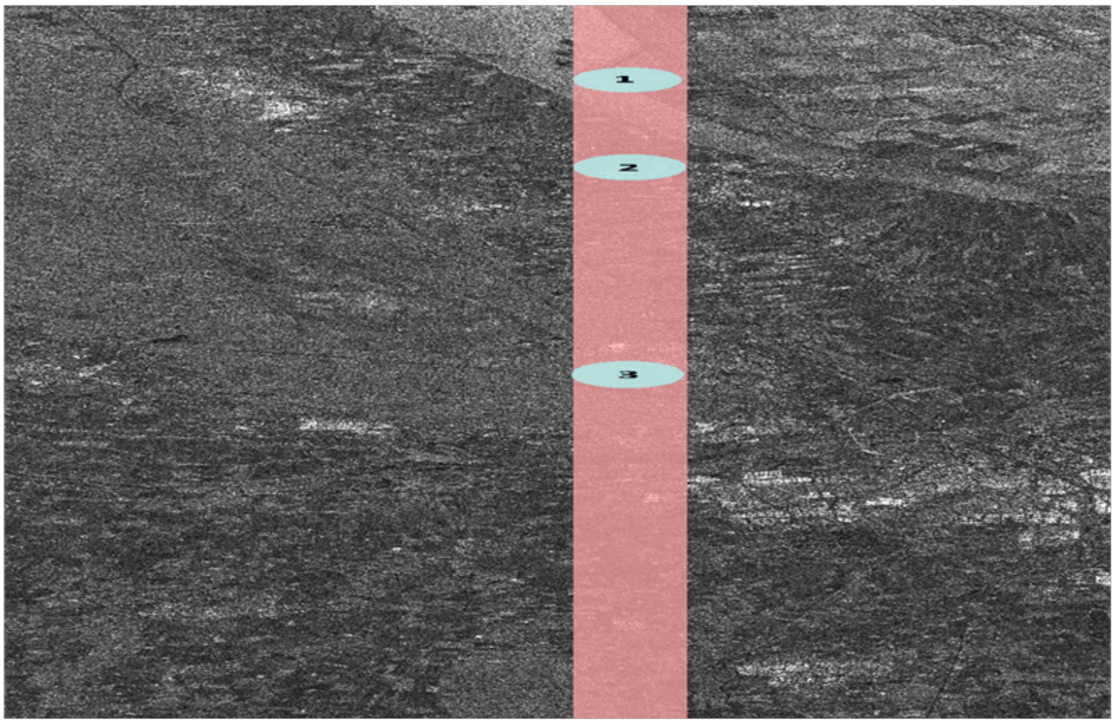


(b)

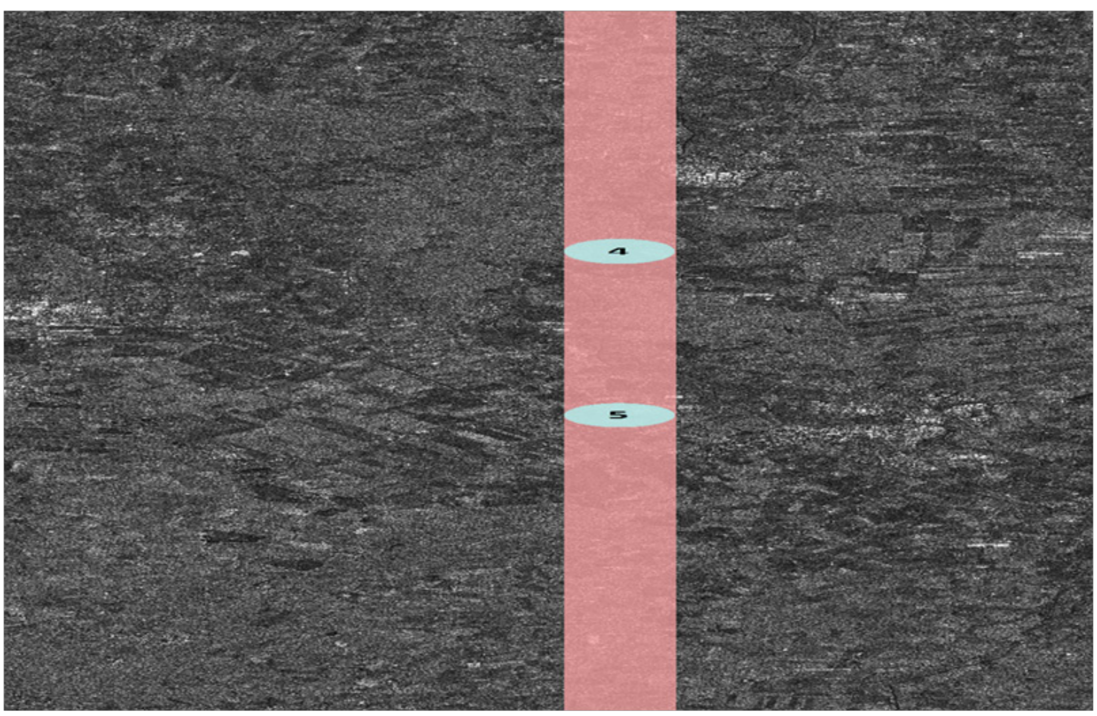


(c)

**Fig. 7:** The scene area a) five segments b) 3 of 5 segment zoomed c) 2 of 5 segments zoomed

The following set of figures exemplifies a number of problems that appeared in some images during their formation and have been overcomed using the proposed algorithm.

The first image in figure8 clearly demonstrates a visible displacement or misalignment between the two halves of the image. This is evident upon examination of the width of the canal, which is noticeably broader in the first image prior to applying the proposed algorithm to correct the displacement caused by the antenna steering. This displacement artifact is also apparent in the lower left region of the image, where it has affected the transfer of certain features outside the image bounds, as indicated by the red circle infigure 8b.

(a)

(b)

(c)

**Fig. 8:** Segment #1 image a) Uncompensated b)Proposed algorithm c) Sentinal-1

Another analysis of the displacement effect on the image is shown in Figure 9, where a bright, shiny target is repeatedly visible within the right red circle. This defect has also introduced the appearance of a feature that was not originally present in the image, as it belonged to the upper preceding segment of the scene area, as denoted by the blue square.

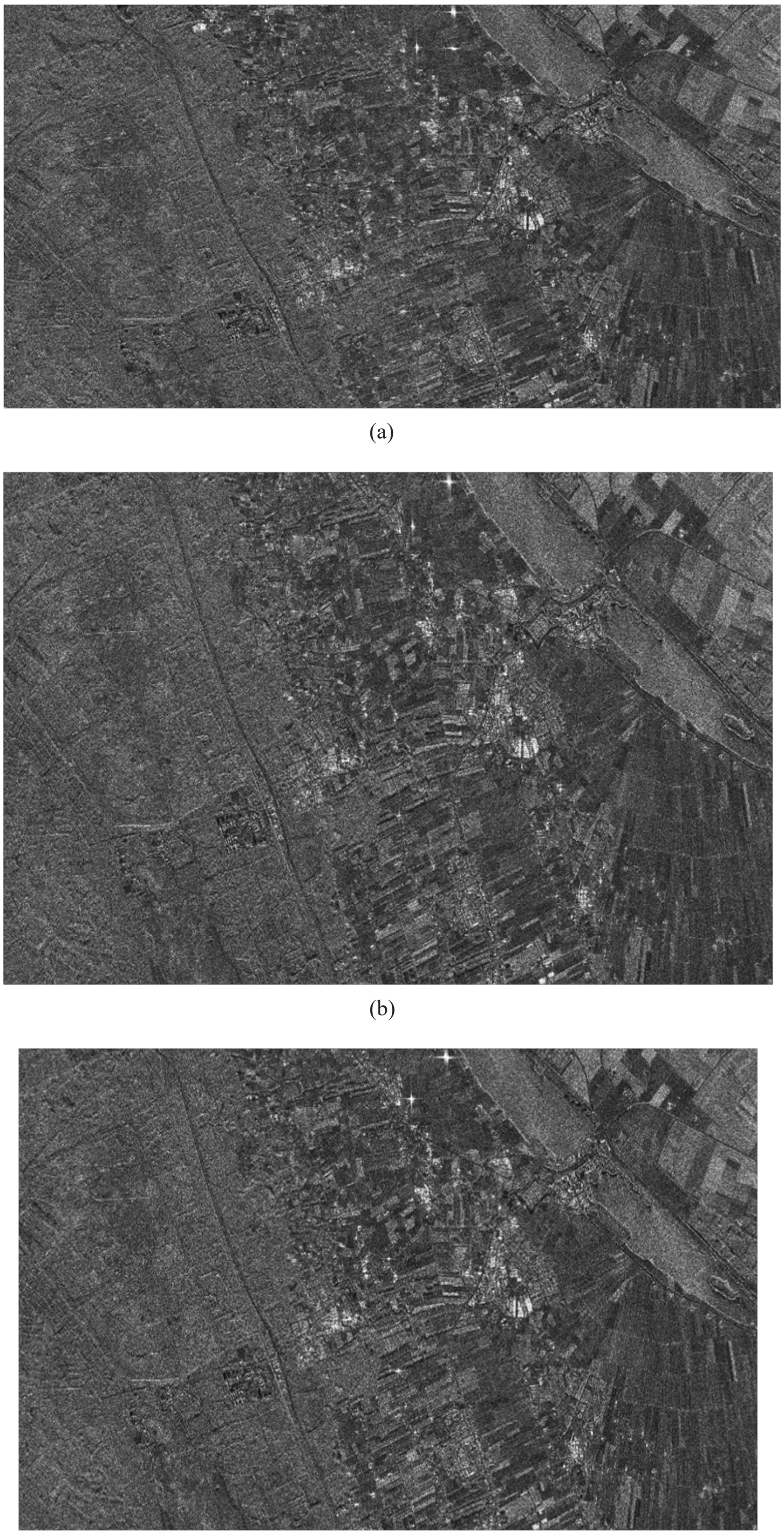

(a)

(b)

(c)

**Fig. 9:** Segment #2 image a) Uncompensated b) Proposed algorithm c) Sentinal-1

Moreover, various errors and defects may happen as the apperence of non present targets or points in the scene area. The first image in figure 10 unambiguously exhibits a pronounced artifact manifesting as a distinct lip or edge, as evidenced by the duplicated or repeated appearance of a single target within the red-encircled region. This observation leaves no room for doubt regarding the presence and characteristics of this antenna-induced aberration. Furthermore, the impact of this artifact on the perceived completeness of the road surface is also clearly visible, as denoted by the red arrows positioned above and below the circled feature, which highlight the associated discontinuities.

In contrast, the second imagein figure 10bpresents a more favorable outcome, wherein the road surface appears complete, as indicated by the two green squares. Additionally, a single, fully resolved target is visible in the foreground, suggesting that the applied algorithmic approach was successful in compensating for the lip artifact and mitigating the errors introduced by the antenna steering process.

(a)

(b)

(c)

**Fig. 10:** Segment #3 image a) Uncompensated b)Proposed algorithm c) Sentinal-1

The disruption of the waterway is clearly visible in multiple locations of figure 11, as indicated by the red arrows. The incomplete nature of the residential area, as pointed out by the red arrow at the bottom left of the image, is also readily apparent and is further illustrated in the subsequent image, which was generated using the algorithm presented and denoted by the green arrow.

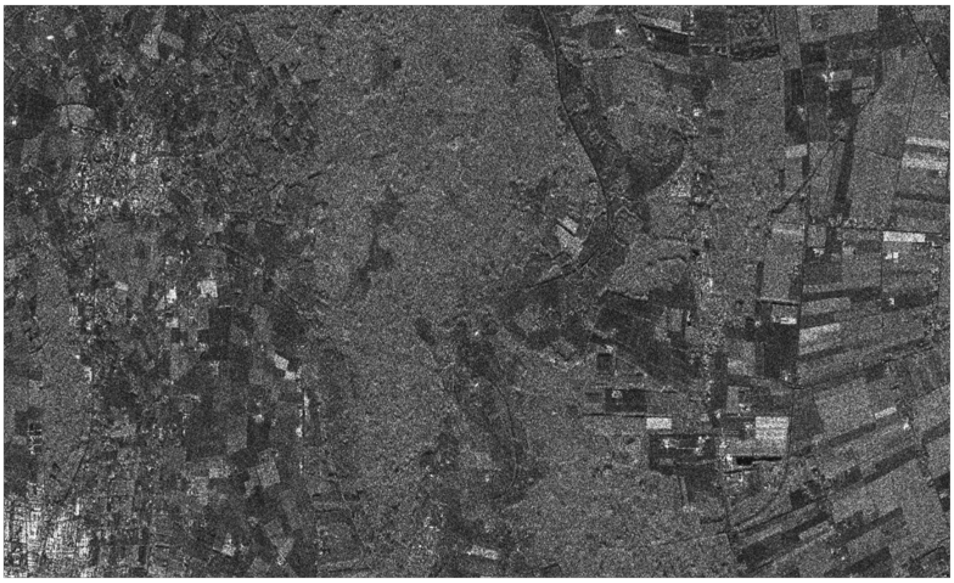

(a)

(b)

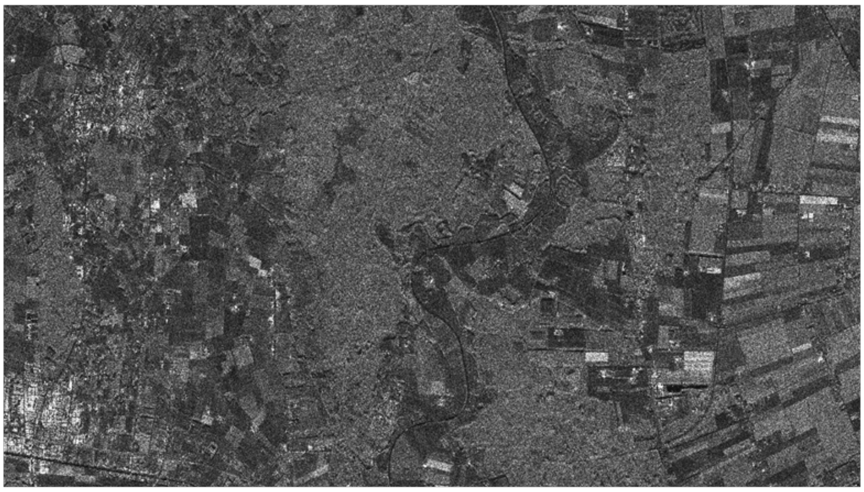

(c)

**Fig. 11:** Segment #4 image a) Uncompensated b) Proposed algorithm c) Sentinal-1

This image, shown in figure12a, requires no additional commentary, as the shadow running along the length of the image clearly contains a break in several parts of the river, as indicated. There is also a truncated section at the bottom left of the image, which corresponds to the portion that appears in the bottom left cornerofthe corrected image Figure 12a and is surrounded by the green frame

(a)

(b)

(c)

**Fig. 12:** Segment #5 image a) Uncompensated b)Proposed algorithm c) Sentinal-1

To further corroborate the visual analysis, verified quantitative metrics were also employed, which confirmed the excellent performance of the proposed methodology and the observations made through the imagery as follows.

First, the contrast of an image is calculated by means of calculating the ratio between the iamge intensity standard deviation and the mean of image intensity, respectively[17].

$$\text{Contrast} = \frac{\sqrt{\mathrm{E}\{[\mathrm{I}^2(\mathrm{m,n}) - \mathrm{E}\{\mathrm{I}^2(\mathrm{m,n})\}]^2\}}}{\mathrm{E}\{\mathrm{I}^2(\mathrm{m,n})\}} \tag{2}$$

$$\mathrm{E}\{\mathrm{I}^2(\mathrm{m,n})\} = \frac{1}{MN}\sum_{m=1}^{M}\sum_{n=1}^{N} I^2(m,n) \tag{3}$$

$$\text{Sharpness} = \sum_{m} Height \sum_{n} Width\ (S_x(m,n)^2 + S_y(m,n)^2) \tag{4}$$

$$\text{Entropy} = -\sum_{m}\sum_{n}\left(\frac{I^2(m,n)}{E_t}\right)\ln\left(\frac{I^2(m,n)}{E_t}\right) \quad (5)$$

$$E_t = -\sum_{m}\sum_{n} I^2(m,n) \quad (6)$$

Mean opinion score (MOS) has become a very popular indicator of perceived media quality. While there is a clear benefit to such a “reference quality indicator” and its widespread acceptance. Most often judged on a scale of 1 (bad) to 5 (excellent), Mean Opinion Scores are the average of a number of other human-scored individual parameters. Although originally Mean Opinion Scores were derived from surveys of expert observers, today a MOS is often produced by an Objective Measurement Method approximating a human ranking[19].

Generically, a Mean Opinion Score can be employed anywhere human subjective experience and opinion is useful. In practice, it is often used to judge digital approximations of world phenomena.

Commonly employed domains where Mean Opinion Score is applied include static image compression (e.g. JPG, GIF), audio codecs (e.g. MP3, Vorbis, AAC, Opus) and video codecs (e.g. H.264, VP8). It is also very commonly employed in streaming sessions where network effects can degrade communications quality.

It is the arithmetic mean over all individual "values on a predefined scale that a subject assigns to his opinion of the performance of a system quality"[20]. Such ratings are usually gathered in a subjective quality evaluation test, but they can also be algorithmically estimated.The opinion of (10) persons was relied upon, including (8) specialists in the field of SAR data / image processing and (2) beginners in the field. The results were as shown in Table 1.

Structural similarity index measure (SSIM) can be used as a benchmark to check the performance of other image progressing algorithms, like image compression. The human visual system is adapted to extract structural information. The SSIM algorithm separates out the similarity measurements into three different components: Luminance, Contrast, and Structural.

The luminance between the two signals is determined by the mean intensity of the signals. The contrast is determined by the standard deviation. And the structural is determined by the correlation of the two signals[21].

$$L(x,y) = (2\mu x\mu y + C1) / (2\mu x2 + \mu y2 + C1) \quad (7)$$

$$C(x,y) = (2\sigma x\sigma y + C2) / (2\sigma x2 + \sigma y2 + C2) \quad (8)$$

$$S(x,y) = (\sigma xy + C3) / (\sigma x\sigma y + C3) \quad (9)$$

Where $\mu x$, $\mu y$ is the mean over a window in Image X, Image Y respectively
$\sigma x$, $\sigma y$ is standard deviation (square root of variance) over a window in Image X, Image Y respectively
$\sigma xy$ is co-variance over a window between Image X and Image Y.
x and y refer to a local window in the Image X and Y respectively, and C1, C2 and C3 are constants.
SSIM (x,y) is a multiplication of these three components.
If C3 is set to C2/2, then over a particular window.

$$SSIM(x,y) = ((2\mu x\mu y + C1) * (2\sigma xy + C2)) / ((\mu x2 + \mu y2 + C1) * (\sigma x2 + \sigma y2 + C2)) \quad (10)$$

The Mean-SSIM is the average over all such local windows. The window is moved across the image one pixel at a time.The value range of SSIM is [0 to 1], where the larger the value, the smaller the image distortion[22].

The standard parameters most commonly used in judging the quality of images were calculated and listed in Table No. 1 below.

**Table 1:** Image Quality Metrics

| **Segment#1** | **Uncompensated** | **Proposed compensation algorithm** | **Sentinel-1** |
|---|---|---|---|
| Entropy | 14.3377 | 14.2282 | 14.2468 |
| Sharpness | 1841.20 | 2185.98 | 1174.05 |
| Contrast | 23.3905 | 24.4998 | 28.9589 |
| SSIM | N/A | 0.97 | |
| MOS | N/A | 4.4 | |
| **Segment#2** | **Uncompensated** | **Proposed compensation algorithm** | **Sentinel-1** |
| Entropy | 13.6825 | 13.6109 | 13.6970 |
| Sharpness | 7232.89 | 6582.15 | 2689.43 |
| Contrast | 47.6567 | 47.5468 | 53.4524 |
| SSIM | N/A | 0.99 | |
| MOS | N/A | 4.9 | |

| Segment#3 | Uncompensated | Proposed compensation algorithm | Sentinel-1 |
|---|---|---|---|
| Entropy | 13.3004 | 13.2585 | 13.1957 |
| Sharpness | 7236.71 | 7569.92 | 3269.58 |
| Contrast | 46.9590 | 47.2653 | 58.1195 |
| SSIM | N/A | 1 | |
| MOS | N/A | 5 | |
| **Segment#4** | **Uncompensated** | **Proposed compensation algorithm** | **Sentinel-1** |
| Entropy | 14.2073 | 14.0664 | 14.1887 |
| Sharpness | 10713.68 | 10737.64 | 10579.33 |
| Contrast | 17.7469 | 23.2857 | 16.4838 |
| SSIM | N/A | 1 | |
| MOS | N/A | 5 | |
| **Segment#5** | **Uncompensated** | **Proposed compensation algorithm** | **Sentinel-1** |
| Entropy | 13.8999 | 13.8587 | 13.9053 |
| Sharpness | 2913.24 | 2924.07 | 2677.91 |
| Contrast | 32.2517 | 32.8617 | 31.9791 |
| SSIM | N/A | 0.96 | |
| MOS | N/A | 4.8 | |

The results presented in this work are compelling. The visual examination and comparison of the images clearly show that the proposed algorithm is able to effectively address the previously identified errors or defects, as indicated by the marked points in each image. The approved and documented measurements further confirm the algorithm's capability, with the post-processing measurements demonstrating significant improvements when compared to the original, unprocessed data.

Importantly, the comparison to Sentinel-1 satellite imagery is quite promising. The key parameters have largely achieved improvement, and in many cases have reached values quite close to that of the Sentinel data. This suggests the proposed approach is able to deliver results on par with established satellite-based monitoring techniques. Overall, these findings strongly support the efficacy and potential of the developed algorithm for addressing the problem at hand.

## 4. Conclusion

This paper introduces a solution to overcome common challenges in synthetic aperture radar (SAR) imaging, such as the effects of shadows, layover, and multipath interference missing or corrupted data in SAR images. This solution for LEO spaceborne SAR, focused on solving the problem of artifacts due to satellite antenna steering via representing two main contributions. First, a motion compensation scheme for the antenna steering is constructed to join with a chirp-scaling algorithm in which analysis and a calculation of platform navigation data are executed. Second, the proposed scheme results are compared with the Sentinel-1 SLC image using two evaluation methods. The first method is executed using Mean Opinion Score (MOS) , structural similarity index measure (SSIM),Moreover, measuring image quality metrics such as entropy, contrast, and sharpness for five different segments in the illuminated area. Finally, a noticeable enhancement in all these parameters is realized with remarkable efficiency as presented in table 1, this represents a significant advancement, as the ability to synthetically produce high-fidelity images that are indistinguishable from authentic sensor data holds tremendous value for a variety of applications, such as data augmentation, scene completion, and the generation of training samples for machine learning models. The authors leveraged advanced generative techniques to achieve this level of photorealistic image synthesis, marking an important milestone in the field of computational imaging.


## 5. Acknowledgments

The authors would like to express their gratitude for the availability of free level-0 and level-1 single-look complex (SLC) Sentinel-1 Synthetic Aperture Radar (SAR) data, which was instrumental in enabling this research. The extensive documentation provided by the European Space Agency (ESA) on the Sentinel-1 mission and data processing was also invaluable in facilitating a clear understanding of the decoding process.

The authors would also like to extend an invitation to researchers interested in obtaining the open-source MATLAB code developed for this study. Interested parties are welcome to contact the first or corresponding author, provided that this paper is properly cited in any subsequent work or publications.


## 6. References


[1] Elbohy, A., Helmy, A.,Mashaly, A.,Azouz, A., 2023. “Spaceborne Synthetic Aperture Radar (SAR) Motion Compensation Using Autofocus”. EJMTC, Egypt 2023, Vol. 8_Issue 1_PP 61-68.

[2] Haris, D., Katmoco, S., Rahmat, A.,2019. "An Analysis of Black Fill Artefacts Noise Removal on GRD ProductsSentinel-1 Data". International Journal on Advanced Science, Engineering and Information Technology.

[3] Anghel, A., Cacoveanu, R., Rommen, B., Datcu, M., 2020. Time-Domain SAR Processor for Sentinel-1 TOPS Data, IGARSS 2020 - 2020 IEEE International Geoscience and Remote Sensing Symposium. pp. 1913-1916.

[4] Sentinel-1Level-1Detailed AlgorithmDefinition., 2022.
[5] D., Geudtner, R., Torres, P., Snoeij, M., Davidson, B., Rommen"Sentinel-1 System Capabilities and Application". 2014. IGARSS, Egypt 2014, IEEE.
[6] Sentinel-1Level-0ProductFormatSpecification 2012.
[7] Sentinel-1ProductDefinition 2016
[8] Azouz, A., Fouad, M., ELbohy, A., Abdalla, A., and Mashaly, A. " SAR image formation scheme implementation and endorsement sprouting from Level-0 data decoding'. The Egyptian Journal of Remote Sensing and Space Science, 26(2), 253-263.
[9] Fouad, M., Elbohy, A., Mashaly, A., Abosekeen, A., Abdalla, A., Azouz, A., 2022. Spaceborne SAR image formation enhancement using MOCO techniques. The Egyptian Journal of Remote Sensing and Space Science 25(3), 659-671.
[10] Pu, W., 2021. Deep SAR Imaging and Motion Compensation. IEEE Trans. ImageProcess. 30, 2232–2247.
[11] Sentinel-1 ESA's Radar Observatory Mission for GMeS Operational Services, 2012
[12] Safy, M., Eltanany, A. S., and Amein, A. S. SAR Images Co-registration Based on Gradient Descent Optimization. convergence, 15(17), 23-29.
[13] Eltanany, A. S., Amein, A. S., and Elwan, M. S. (2021). A modified corner detector for SAR images registration. International Journal of Engineering Research in Africa, 53, 123-156.
[14] Cruz, H., Véstias, M., Monteiro, J., Neto, H., Duarte, R.P., 2022. A Review of Synthetic-Aperture Radar Image Formation Algorithms and Implementations: A Computational Perspective. Remote Sensing 14(5), 1258.
[15] Johnsen, H., Piantanida, R., Hajduch, G., 2021. Sentinel-1 Product Specification forproducts generated with IPF 3.4.0.
[16] M. Sakr, A. Saleh, F. AbdElkader, G. Amer, and M. AboElenean, "Enhanced synthetic aperture radar image autofocus and classification using 2D SARNet framework," Journal of Applied Remote Sensing, vol. 18, pp. 026507 - 026507, 2024.
[17] Elbohy, A., Azouz, A., Mashaly, A., Helmy, A., 2023. "Evaluating the Effect of Stage Removal on the Performance of Phase Gradient Autofocus (PGA) Algorithm". ITC, Egypt 2023, IEEE.
[18] Azouz, A.A.E., Li, Z., "Improved phase gradient autofocus algorithm based on segments of variable lengths and minimum-entropy phase correction". IET Radar, Sonar and Navigation 2015.9(4), 467-479.
[19] S. Robert and W. Stefan and H. David. "Mean opinion score (MOS) revisited: methods and applications, limitations and alternatives". Multimedia Systems. 2016 22. 213-227.
[20] Streijl, Robert C., S.Winkler and David S. "Mean opinion score (MOS) revisited: methods and applications, limitations and alternatives." Multimedia Systems 22 2016: 213-227.
[21] I. Bakurov, M. Buzzelli, R.Schettini, M. Castelli, L. Vanneschi, "Structural similarity index (SSIM) revisited: A data-driven approach, Expert Systems with Applications" Volume 189, 2022.
[22] S. Umme and A. Morium, M Shorif. "Image Quality Assessment through FSIM, SSIM, MSE and PSNR—A Comparative Study". Journal of Computer and Communications. 07. 8-18. (2019).